

Using adaptiveness and causal superpositions against noise in quantum metrology

Stanisław Kurdziałek,^{1,*} Wojciech Górecki,^{1,*} Francesco Albarelli,^{2,3} and Rafał Demkowicz-Dobrzański¹

¹*Faculty of Physics, University of Warsaw, Pasteura 5, 02-093 Warszawa, Poland*

²*Dipartimento di Fisica “Aldo Pontremoli”, Università degli Studi di Milano, via Celoria 16, 20133 Milan, Italy*

³*Istituto Nazionale di Fisica Nucleare, Sezione di Milano, via Celoria 16, 20133 Milan, Italy*

We derive new bounds on achievable precision in the most general adaptive quantum metrological scenarios. The bounds are proven to be asymptotically saturable and equivalent to the known parallel scheme bounds in the limit of large number of channel uses. This completely solves a long standing conjecture in the field of quantum metrology on the asymptotic equivalence between parallel and adaptive strategies. The new bounds also allow to easily assess the potential benefits of invoking non-standard causal superposition strategies, for which we prove, similarly to the adaptive case, the lack of asymptotic advantage over the parallel ones.

Introduction. In the field of quantum information and quantum technologies, one can distinguish three levels of *quantumness* that are behind the boost in performance of various communication [1, 2], computational [3] or metrological tasks [4–6]. The most rudimentary one is *quantum coherence* (C), which refers to the potential of having a single quantum system in the state of quantum superposition. This is already enough to implement secure quantum key distribution protocols [7] or even reach the Heisenberg limit in noiseless quantum metrology, provided a given quantum probe can pass through a sensing channel multiple times [8, 9]. The next level is *entanglement* (E), where quantum coherence present in multi-partite systems manifests itself in the form of non-classical correlations. This quantumness level is crucial to guarantee quantum speed-up in computational tasks [10] as well as to assure the ultimate security in the so-called device-independent quantum key distribution [11]. In quantum metrology, it had long been appreciated as the way to boost the precision in optical and atomic interferometric tasks [12–16], either in the form of somehow overhyped N00N states [17, 18] or much more practical optical and atomic squeezed states [19, 20]. Finally, exploiting the quantum potential to its limits, one can consider *adaptive* (AD) or *active quantum feedback* strategies, where the probes are entangled with noiseless ancillary systems, and quantum control operations may actively modify the probe system that will be sent to the subsequent channel based on the information obtained so far [21–25], see Fig. 1. Such protocols represent the most general channel sensing schemes, containing (E) as a special case and encompassing in particular all quantum error-correcting strategies widely used in the whole field of quantum information processing to counter noise [26–29].

Interestingly, in the absence of noise, (AD) strategies provide no advantage over optimal (E) strategies [30]. In the presence of noise, however, some advantages have been observed in the small-number-of-uses regime where a direct search of optimal metrological protocols could be

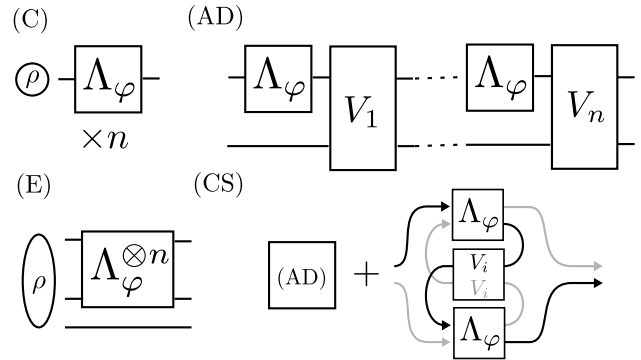


FIG. 1. Metrological schemes utilizing “four levels of quantumness”: (C) channels probed independently (basic use of quantum coherence); (E) channels probed in parallel using a general entangled state, with ancillary systems potentially involved; (AD) general adaptive (active quantum feedback) strategies; (CS) causal superposition strategies, where additionally channels may be probed in a superposition of different causal orders.

carried out [21, 31–35]. In 2014 a conjecture has been formulated [21] predicting no asymptotic advantage of (AD) over (E). A notable progress in answering this fundamental question has been made in 2021 [36, 37], when it was demonstrated that in the models where quantum coherence cannot be protected against noise on arbitrary scale, and hence the Heisenberg scaling (HS) is not achievable, (AD) strategies offer no asymptotic advantage over (E). Still, the full answer to the question was lacking, mainly due to the fact that the bounds used there were not tight enough.

In this paper, utilizing our new bounds, we indeed answer the conjecture in an affirmative way, proving in full generality that (AD) strategies provide no asymptotic advantage over (E). As negative as it may sound, the result by no means implies that (AD) strategies are useless. In fact, our bounds allow to clearly pinpoint the potential advantage one may expect in the finite number-of-uses regime, and easily observe how the advantage fades away when approaching the asymptotic limit of large number of channel uses. On a more practical side, adaptive strategies may sometimes be in fact easier to implement

* These two authors contributed equally to the project.

than parallel, as they may not necessarily require entangling large number of particles, while obtaining the same effect via small scale entanglement + active feedback.

Even though the “three levels of quantumness” listed above appear to cover all quantum aspects of metrological protocols, an intriguing idea was put forward of considering *causal superposition strategies* (CS) where different channels are being probed in a superposition of different causal orders [35, 38–44]. Advantages of such a strategy over the most general (AD) strategy have been observed, but no efficiently computable bounds have been proposed. In this paper, we provide bounds valid also for this more general class of protocols and show their asymptotic equivalence to (AD) and (E), which also means that (CS) strategies cannot surpass the HS [45].

Introductory example. Let us start with the most elementary yet very illuminating example of a noisy metrological model, where it is possible to remove noise while assuring the preservation of HS of precision in the asymptotic regime. Consider a single qubit channel $\Lambda_\varphi(\cdot) = \sum_k K_{\varphi,k} \cdot K_{\varphi,k}^\dagger$, where $K_{\varphi,k} = U_\varphi K_k$,

$$U_\varphi = e^{-\frac{i}{2}\sigma_z\varphi}, \quad K_1 = \sqrt{p}\mathbb{1}, \quad K_2 = \sqrt{1-p}\sigma_x. \quad (1)$$

The channel represents dephasing of a qubit along the x axis of the Bloch ball (the operator K_2 may be understood as a σ_x error occurring with probability $1-p$) and the subsequent rotation U_φ of the state around the z axis by angle φ , where φ is the parameter to be estimated—a similar model has been used in an experimental demonstration of quantum error-correction enhanced metrology in NV-center sensing setups [46], as well as in [47] where the possibility of beating the standard scaling (SS) in presence of transversal noise was shown. In case of a single channel use, $n=1$, the effect of noise may be completely mitigated by choosing the input state as $|\psi^{(1)}\rangle = |+\rangle = (|0\rangle + |1\rangle)/\sqrt{2}$. This state is not affected by σ_x error and the output state $|\psi_\varphi\rangle = (|0\rangle + e^{i\varphi}|1\rangle)/\sqrt{2}$ represents a noiseless phase encoding. We will quantify the performance of a given protocol using the *quantum Fisher information* (QFI) [48, 49] of the output state, which in this case is $F^{(1)} = 1$ (we recall the definition of the QFI in Appendix A).

Assume now that we can use the channel twice, $n=2$. If we send the optimal single qubit probes independently to each of the channels, we get the QFI value $F_C^{(2)} = 2$. We can, however, also consider a parallel strategy involving an entangled input state $|\psi^{(2)}\rangle = (|00\rangle + |11\rangle)/\sqrt{2}$ (the N00N state). In this case if either zero or two σ_x error occur, the final state will again correspond to the noiseless phase encoding $|\psi_\varphi^{(2)}\rangle = U_\varphi^2 |\psi^{(2)}\rangle = (|00\rangle + e^{2i\varphi}|11\rangle)/\sqrt{2}$ for which the QFI equals 4. Whereas, if only a single σ_x occurs the state will contain no information about the phase at all. As a result the final QFI reads $F_E^{(2)} = 4(p^2 + (1-p)^2) \geq F_C^{(2)}$. Interestingly, this result may be further improved via a simple adaptive strategy. The protocol involves entangling the initial single probe qubit with a single ancillary qubit, so

that the input state is again $|\psi^{(2)}\rangle$. After a single action of the channel, $\Lambda_\varphi \otimes \mathcal{I}$, an error correction operation is performed, where we check if a σ_x error occurred and correct the error accordingly. Then the channel acts on the probe state again, and with probability p yields the ideal state $|\psi_\varphi^{(2)}\rangle$, while if another σ_x error occurs, the final unitary rotation U_φ removes all the phase information from the state. Consequently, the protocol yields a QFI equal to $4p$. This protocol is actually the optimal one provided $p \geq 0.5$. If $p < 0.5$, then one simply needs to modify the recovery operation in a way that instead of correcting a single σ_x error on the probe system the σ_x operation is applied to the ancillary qubit. In the end the optimal QFI reads $F_{AD}^{(2)} = 2(1 + |1 - 2p|) \geq F_E^{(2)}$ (see Appendix A for details).

With this example in mind, one may wonder how to prove that the actual protocols are indeed optimal and what is (if any) the potential benefit of using even more general causal superposition strategies, $F_{CS}^{(2)} = ?$. For larger n the task becomes even more challenging, and no brute-force optimization approach can tell what happens in the asymptotic limit $n \rightarrow \infty$. The methods developed in this paper allow to answer all these questions.

State-of-the-art bounds. The most powerful state-of-the-art bounds for the performance of (E) as well as (AD) strategies, are based on the concept of minimization of certain operator norm expressions over different Kraus representation of the channel $\Lambda_\varphi = \sum_k K_{\varphi,k} \cdot K_{\varphi,k}^\dagger$ [21, 22, 28, 31, 37, 50–53]—in what follows we drop subscript φ in Kraus operators for conciseness. For (E) strategies, the upper bound on the achievable QFI, reads:

$$F_E^{(n)} \leq \min_{\{K_k\}} 4 [n\|\alpha\| + n(n-1)\|\beta\|^2], \quad (2)$$

where $\|\cdot\|$ denotes the operator norm, $\alpha = \sum_k \dot{K}_k^\dagger \dot{K}_k$, $\beta = \sum_k \dot{K}_k^\dagger K_k$ and $\dot{K}_k = \partial_\varphi K_k$. If a Kraus representation exists for which $\beta = 0$, the QFI scales asymptotically at most linearly with n —SS models—and the optimal quantum enhancement amounts to a constant factor improvement [21, 51–53]. If no such representation exists, then the HS can be preserved asymptotically [28, 37]. Interestingly, the above bound has been proven to be asymptotically tight for both SS ($\beta = 0$) and HS ($\beta \neq 0$) models [37].

Moving to (AD) strategies, the best state-of-the-art universally valid bound reads [21, 31, 37]:

$$F_{AD}^{(n)} \leq \min_{\{K_i\}} 4 \left[n\|\alpha\| + n(n-1)\|\beta\| \left(\|\beta\| + 2\sqrt{\|\alpha\|} \right) \right]. \quad (3)$$

It is asymptotically equivalent to the parallel bound, Eq. (2), in case of SS models ($\beta = 0$), and, since the parallel bound is asymptotically saturable, this implies no asymptotic advantage of (AD) strategies over (E). Still, the bound leaves space for improvement for finite n and does not exclude an asymptotic advantage for HS

models—the term quadratic in n has a larger coefficient than the one in Eq. (2).

Iterative bound. Below, we derive a tighter adaptive bound than the one given above, and prove it is asymptotically equivalent to the parallel one—consequently, this implies no asymptotic advantage of (AD) over (E) for all models (both SS and HS).

Let $\Lambda_\varphi^{(n)}(\cdot) = \sum_{\mathbf{k}^{(n)}} K_{\mathbf{k}^{(n)}} \cdot K_{\mathbf{k}^{(n)}}^\dagger$ represent a combined action of n channels Λ_φ in a general adaptive strategy where they are intertwined with control operations V_i acting on probe and ancillary systems, as in Fig. 1(AD). $K_{\mathbf{k}^{(n)}}$ denote the corresponding Kraus operators, which can be computed via the following iteration relation: $K_{\mathbf{k}^{(1)}} = V_1(K_{k_1} \otimes \mathbb{1})$,

$$K_{\mathbf{k}^{(i+1)}} = V_{i+1}(K_{k_{i+1}} \otimes \mathbb{1})K_{\mathbf{k}^{(i)}}, \quad (4)$$

where $\mathbf{k}^{(i)} = (k_i, \dots, k_1)$, and $\mathbb{1}$ is acting on the ancillary system (we will drop it in what follows for conciseness of notation).

The starting point for the derivation of the state-of-the-art bounds as reported in Eqs. (2,3), is an observation that, given a channel $\Lambda_\varphi^{(n)}$, maximization of the QFI of the output state over all inputs and sets of control operations can be upper bounded by [50]:

$$F_{\text{AD}}^{(n)} = \max_{\rho_0, \{V_i\}} F \left[\Lambda_\varphi^{(n)}(\rho_0) \right] \leq \max_{\{V_i\}} \min_{\{K_{\mathbf{k}^{(n)}}\}} 4 \left\| \alpha^{(n)} \right\|, \quad (5)$$

where $\alpha^{(n)} = \sum_{\mathbf{k}^{(n)}} \dot{K}_{\mathbf{k}^{(n)}}^\dagger \dot{K}_{\mathbf{k}^{(n)}}$, the minimization is performed over all equivalent Kraus representations of $\Lambda_\varphi^{(n)}$ and $\|\cdot\|$ is the operator norm. Note that for large enough ancillary system the inequality becomes equality. As such, this inequality is not of much practical use due to infeasibility of performing the minimization over all Kraus representations for larger values of n , as well as the need to additionally perform the optimization over the control operations V_i . The usefulness of this inequality stems from the fact, that it is possible to further upper bound the r.h.s. of Eq. (5) with norms of operators defined in terms of Kraus operators of the *elementary channel* Λ_φ . This is how bounds (2,3) were obtained [21, 31, 37, 51, 52].

In what follows we provide a novel step-by-step approach, where at each step we bound the maximal *increase* in the final QFI thanks to the additional usage of a single quantum channel [54]. Using Eq. (4) we have

$$\begin{aligned} \alpha^{(i+1)} &= \sum_{k_{i+1}, \mathbf{k}^{(i)}} \left(K_{\mathbf{k}^{(i)}}^\dagger \dot{K}_{k_{i+1}}^\dagger + \dot{K}_{\mathbf{k}^{(i)}}^\dagger K_{k_{i+1}}^\dagger \right) \times \text{h.c.} \\ &= \sum_{\mathbf{k}^{(i)}} K_{\mathbf{k}^{(i)}}^\dagger \alpha K_{\mathbf{k}^{(i)}} + K_{\mathbf{k}^{(i)}}^\dagger \beta \dot{K}_{\mathbf{k}^{(i)}} + \dot{K}_{\mathbf{k}^{(i)}}^\dagger \beta^\dagger K_{\mathbf{k}^{(i)}} + \alpha^{(i)}. \end{aligned} \quad (6)$$

We will now use the following operator norm inequality

(see Appendix B for the proof):

$$\left\| \sum_k L_k^\dagger A Q_k \right\| \leq \sqrt{\left\| \sum_k L_k^\dagger L_k \right\|} \|A\| \sqrt{\left\| \sum_k Q_k^\dagger Q_k \right\|}, \quad (7)$$

which, together with the triangle inequality and the trace preservation condition, $\sum_{\mathbf{k}^{(i)}} K_{\mathbf{k}^{(i)}}^\dagger K_{\mathbf{k}^{(i)}} = \mathbb{1}$, yields:

$$\|\alpha^{(i+1)}\| \leq \|\alpha^{(i)}\| + \|\alpha\| + 2\|\beta\| \sqrt{\|\alpha^{(i)}\|}. \quad (8)$$

Let us define the following iteration,

$$a^{(i+1)} = a^{(i)} + \|\alpha\| + 2\|\beta\| \sqrt{a^{(i)}}, \quad a^{(0)} = 0, \quad (9)$$

which, in light of Eq. (5,8), yields $F_{\text{AD}}^{(n)} \leq 4a^{(n)}$. The resulting bound $4a^{(n)}$ may be optimized over the choice of Kraus representation of the elementary channel in each iteration *separately* (how to efficiently implement this iteration numerically is described in Appendix D) or, in a weaker variant, over a *single* Kraus representation identically used in each step (for which the resulting bound will also be valid for (CS) strategies—see Appendix C for the proof). Since $a^{(n)}$ is strategy-independent, the maximization over $\{V_i\}$, or, more generally, over all (CS) strategies, is no longer necessary. This finally yields

$$F_{\text{AD}}^{(n)} \leq \min_{\{K_k\}^{\times n}} 4a^{(n)}, \quad F_{\text{CS}}^{(n)} \leq \min_{\{K_k\}} 4a^{(n)}. \quad (10)$$

Interestingly, the possibility to use a different Kraus representation for each channel use allows to tighten the bound also for parallel strategies, see Appendix D 3.

Closed formula bounds. In order to appreciate how much tighter the obtained bounds are compared to the state-of-the-art bounds, we will provide some closed formulas for the bounds that result from a relaxed variants of the iteration procedure. First, observe that from Eq. (7) we get $\|\beta\| \leq \sqrt{\|\alpha\|}$. From Eq. (9) it then follows that $a^{(n)} \leq n^2 \|\alpha\|$ (the bound obtained in [34]), which when put back into the iteration formula results in

$$F_{\text{AD,CS}}^{(n)} \leq \min_{\{K_k\}} 4 \left(n \|\alpha\| + n(n-1) \|\beta\| \sqrt{\|\alpha\|} \right). \quad (11)$$

Note, that the bound is noticeably tighter than Eq. (3) and is also valid for (CS) strategies, as the same Kraus representation is used in each step. We also see that the difference between this bound and Eq. (2) amounts to replacing one $\|\beta\|$ with $\sqrt{\|\alpha\|}$. It might be tempting to conjecture that this difference represents in fact the asymptotic gain of (AD) over (E) strategies. This is not the case, however, as we demonstrate below.

For any fixed $\|\alpha\|, \|\beta\|$ consider the following function $f(n) = n\|\alpha\| + n(n-1)\|\beta\|^2 + n \log n (\|\alpha\| - \|\beta\|^2)$. For $n \geq 0$ it can be shown (see Appendix E) that $f(n+1) \geq f(n) + \|\alpha\| + 2\|\beta\| \sqrt{f(n)}$. Hence, in light of Eq. (9) we get $f(n) \geq a^{(n)}$ and as a result:

$$F_{\text{AD,CS}}^{(n)} \leq \min_{\{K_k\}} 4 \left[n \|\alpha\| + n(n-1) \|\beta\|^2 \left(1 + \frac{c \log n}{n-1} \right) \right], \quad (12)$$

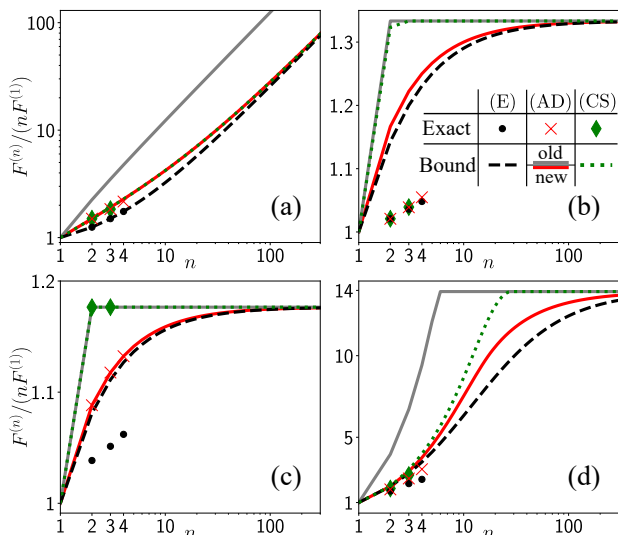


FIG. 2. Achievable QFI as a function of number of channels probed for parallel (E, black), adaptive (AD, red), and causal superposition strategies (CS, green) normalized by n times the single-channel QFI. Points represent the result of the exact optimization, while curves represent the respective bounds. The best previously known adaptive bound (gray) is depicted for comparison. The four plots correspond to different metrological models with a qualitatively different behaviour: (a) dephasing perpendicular to the signal, Eq. (1) ($p = 0.75$); (b) dephasing parallel to the signal, Eq. (14) ($p = 0.75$); (c) damping perpendicular to the signal, Eq. (15) ($p = 0.15$); (d) damping parallel to the signal, Eq. (16) ($p = 0.75$).

where $c = (\|\alpha\| - \|\beta\|^2) / \|\beta\|^2$. Since we know that the parallel bound, Eq. (2), is asymptotically saturable this implies that:

$$\lim_{n \rightarrow \infty} \left(F_{\text{AD,CS}}^{(n)} / F_{\text{E}}^{(n)} \right) = 1 \quad (13)$$

and, hence, there is *no asymptotic advantage* of (AD) nor (CS) over (E).

Interestingly, lack of asymptotic advantage thanks to adaptiveness has also been demonstrated for continuous-time models [25], a result which can be regarded as a limiting case of the theory we develop here (see Appendix F for details).

Examples. In order to illustrate the practical applications of the bounds, we compute them for four representative models and compare the results with the actual performance of the optimal protocols that can be determined numerically for small number of channel uses ($n \leq 4$) via semidefinite programming (SDP) as described in [21] (parallel strategies), [33] (adaptive protocols) and [35] (causal superposition protocols). The results are presented in Fig. 2. As a figure-of-merit we plot the achievable QFI with n uses of a channel normalized by n times $F^{(1)}$ (the maximal QFI for single-channel sensing with a possible use of ancillary systems).

Fig. 2(a) presents results corresponding to the introductory example of perpendicular dephasing model,

Eq. (1)—in all the models that follow we also assume the convention that $K_{\varphi,k} = U_{\varphi} K_k$ (signal comes after noise). Among the four models presented, this is the only one that admits asymptotic HS—hence the linear increase of the figure of merit. Interestingly, the bounds are saturated for $n = 2$ and the optimal QFI values are equal to the ones obtained for the protocols discussed in the introductory example, proving they are indeed optimal. For larger n , the bounds are very tight, and, as expected, the bounds for (AD) and (CS) converge asymptotically to the (E) bound (unlike the state-of-the-art bound).

Results depicted in Fig. 2(b) refer to the parallel dephasing model (both the unitary encoding and the dephasing are with respect to the z axis), where the Kraus operators read:

$$K_1 = \sqrt{p}\mathbb{1}, \quad K_{\varphi,2} = \sqrt{1-p}\sigma_z. \quad (14)$$

In this case, gains due to adaptiveness or causal superpositions are very modest, and the bounds are not particularly tight for low n —still, thanks to the general theorem, we know they are tight asymptotically.

Fig 2(c) illustrates results for the perpendicular amplitude damping model (unitary encoding with respect to the z axis, amplitude damping with respect to the x axis):

$$K_1 = |-\rangle \langle -| + \sqrt{p}|+\rangle \langle +|, \quad K_2 = \sqrt{1-p}|-\rangle \langle +|, \quad (15)$$

where $|\pm\rangle = (|0\rangle \pm |1\rangle) / \sqrt{2}$ are the eigenvectors of σ_x . This model is of particular interest as the finite- n bounds are saturated here both for (AD) and (CS) for all n . This suggests that it is highly unlikely that any tighter metrological bounds can be derived solely from the properties of the single-channel Kraus operators.

Finally, Fig. 2(d) depicts results for the parallel amplitude damping model with:

$$K_1 = |0\rangle \langle 0| + \sqrt{p}|1\rangle \langle 1|, \quad K_2 = \sqrt{1-p}|0\rangle \langle 1|. \quad (16)$$

This model illustrates particularly well how much tighter the novel bounds are, when compared with the previous state-of-the-art ones.

Conclusions and open problems. With the results presented in this paper, we dare to say that the theory of single-parameter quantum metrology in presence of uncorrelated noise is now complete. Universal asymptotically saturable bounds are known as well as efficiently computable bounds in the regime of finite (but potentially large) number of channel uses. This, together with exact algorithms to find optimal protocols for small n , provides a complete landscape of achievable quantum enhancement in realistic quantum metrology. This said, we need to admit that in case of multiparameter models [55, 56], Bayesian models [57, 58], and most importantly models involving temporally or spatially correlated noise [33, 59–62] the quest for a full understanding of quantum metrological potential is still not complete. Nevertheless, these achievements compare favourably to

the ones obtained in the related field of (binary) quantum channel discrimination [63, 64]. Interestingly, adaptive strategies are not useful asymptotically for asymmetric hypothesis testing [65–67], while an advantage is possible in the symmetric setting [68, 69]. However, easily computable asymptotic bounds, as well as practical strategies to attain them for arbitrary channels are still missing,

unlike in quantum metrology. Moreover, the asymptotic analysis of causal superposition strategies for quantum channel discrimination [44, 70] is still an open question.

Acknowledgements. This work was supported by the National Science Center (Poland) grant No.2020/37/B/ST2/02134. FA acknowledges financial support from MUR under the “PON Ricerca e Innovazione 2014-2020” project EEQU.

-
- [1] N. Gisin and R. Thew, Quantum communication, *Nat. Photonics* **1**, 165 (2007).
- [2] F. Xu, X. Ma, Q. Zhang, H.-K. Lo, and J.-W. Pan, Secure quantum key distribution with realistic devices, *Rev. Mod. Phys.* **92**, 025002 (2020).
- [3] J. Preskill, Quantum Computing in the NISQ era and beyond, *Quantum* **2**, 79 (2018).
- [4] V. Giovannetti, S. Lloyd, and L. Maccone, Advances in quantum metrology, *Nat. Photonics* **5**, 222 (2011).
- [5] C. L. Degen, F. Reinhard, and P. Cappellaro, Quantum sensing, *Rev. Mod. Phys.* **89**, 035002 (2017).
- [6] S. Pirandola, B. R. Bardhan, T. Gehring, C. Weedbrook, and S. Lloyd, Advances in photonic quantum sensing, *Nat. Photonics* **12**, 724 (2018).
- [7] C. H. Bennett and G. Brassard, Quantum cryptography: Public key distribution and coin tossing, in *Proceedings of the IEEE International Conference on Computers, Systems and Signal Processing* (1984) pp. 175–179.
- [8] B. L. Higgins, D. W. Berry, S. D. Bartlett, H. M. Wiseman, and G. J. Pryde, Entanglement-free heisenberg-limited phase estimation, *Nature* **450**, 393 (2007).
- [9] D. Braun, G. Adesso, F. Benatti, R. Floreanini, U. Marzolino, M. W. Mitchell, and S. Pirandola, Quantum-enhanced measurements without entanglement, *Rev. Mod. Phys.* **90**, 035006 (2018).
- [10] R. Jozsa and N. Linden, On the role of entanglement in quantum-computational speed-up, *Proc. R. Soc. Lond. A* **459**, 2011 (2003).
- [11] A. Acín, N. Brunner, N. Gisin, S. Massar, S. Pironio, and V. Scarani, Device-independent security of quantum cryptography against collective attacks, *Phys. Rev. Lett.* **98**, 230501 (2007).
- [12] S. F. Huelga, C. Macchiavello, T. Pellizzari, A. K. Ekert, M. B. Plenio, and J. I. Cirac, Improvement of frequency standards with quantum entanglement, *Phys. Rev. Lett.* **79**, 3865 (1997).
- [13] L. Pezzé and A. Smerzi, Entanglement, nonlinear dynamics, and the heisenberg limit, *Phys. Rev. Lett.* **102**, 100401 (2009).
- [14] R. Demkowicz-Dobrzański, M. Jarzyna, and J. Kołodyński, Quantum Limits in Optical Interferometry, in *Progress in Optics, Volume 60*, edited by E. Wolf (Elsevier, Amsterdam, 2015) pp. 345–435, arXiv:1405.7703.
- [15] J. P. Dowling and K. P. Seshadreesan, Quantum optical technologies for metrology, sensing, and imaging, *J. Lightwave Technol.* **33**, 2359 (2015).
- [16] L. Pezzè, A. Smerzi, M. K. Oberthaler, R. Schmied, and P. Treutlein, Quantum metrology with nonclassical states of atomic ensembles, *Rev. Mod. Phys.* **90**, 035005 (2018).
- [17] J. J. Bollinger, W. M. Itano, D. J. Wineland, and D. J. Heinzen, Optimal frequency measurements with maximally correlated states, *Phys. Rev. A* **54**, R4649 (1996).
- [18] J. P. Dowling, Quantum optical metrology – the lowdown on high-n00n states, *Contemp Phys* **49**, 125 (2008).
- [19] C. M. Caves, Quantum-mechanical noise in an interferometer, *Phys. Rev. D* **23**, 1693 (1981).
- [20] R. Schnabel, Squeezed states of light and their applications in laser interferometers, *Phys. Rep.* **684**, 1 (2017).
- [21] R. Demkowicz-Dobrzański and L. Maccone, Using Entanglement Against Noise in Quantum Metrology, *Phys. Rev. Lett.* **113**, 250801 (2014).
- [22] R. Demkowicz-Dobrzański, J. Czajkowski, and P. Sekatski, Adaptive Quantum Metrology under General Markovian Noise, *Phys. Rev. X* **7**, 041009 (2017).
- [23] S. Pang and A. N. Jordan, Optimal adaptive control for quantum metrology with time-dependent Hamiltonians, *Nat. Commun.* **8**, 14695 (2017).
- [24] S. Pirandola and C. Lupo, Ultimate precision of adaptive noise estimation, *Phys. Rev. Lett.* **118**, 100502 (2017).
- [25] K. Wan and R. Lasenby, Bounds on adaptive quantum metrology under Markovian noise, *Phys. Rev. Research* **4**, 033092 (2022).
- [26] D. Kribs, R. Laflamme, and D. Poulin, Unified and generalized approach to quantum error correction, *Phys. Rev. Lett.* **94**, 180501 (2005).
- [27] B. M. Terhal, Quantum error correction for quantum memories, *Rev. Mod. Phys.* **87**, 307 (2015).
- [28] S. Zhou, M. Zhang, J. Preskill, and L. Jiang, Achieving the Heisenberg limit in quantum metrology using quantum error correction, *Nat. Commun.* **9**, 78 (2018).
- [29] D. Layden, S. Zhou, P. Cappellaro, and L. Jiang, Ancilla-free quantum error correction codes for quantum metrology, *Phys. Rev. Lett.* **122**, 040502 (2019).
- [30] V. Giovannetti, S. Lloyd, and L. Maccone, Quantum metrology, *Phys. Rev. Lett.* **96**, 010401 (2006).
- [31] P. Sekatski, M. Skotiniotis, J. Kołodyński, and W. Dür, Quantum metrology with full and fast quantum control, *Quantum* **1**, 27 (2017).
- [32] Y. Yang, Memory Effects in Quantum Metrology, *Phys. Rev. Lett.* **123**, 110501 (2019).
- [33] A. Altherr and Y. Yang, Quantum Metrology for Non-Markovian Processes, *Phys. Rev. Lett.* **127**, 060501 (2021).
- [34] J. L. Pereira, L. Banchi, and S. Pirandola, Bounding the benefit of adaptivity in quantum metrology using the relative fidelity, *Phys. Rev. Lett.* **127**, 150501 (2021).
- [35] Q. Liu, Z. Hu, H. Yuan, and Y. Yang, Optimal non-asymptotic quantum metrology with hierarchical strategies, arXiv:2203.09758 (2022).
- [36] S. Zhou and L. Jiang, Optimal approximate quantum

- error correction for quantum metrology, *Phys. Rev. Res.* **2**, 013235 (2020).
- [37] S. Zhou and L. Jiang, Asymptotic Theory of Quantum Channel Estimation, *PRX Quantum* **2**, 010343 (2021).
- [38] M. Araújo, F. Costa, and i. c. v. Brukner, Computational advantage from quantum-controlled ordering of gates, *Phys. Rev. Lett.* **113**, 250402 (2014).
- [39] C. Mukhopadhyay, M. K. Gupta, and A. K. Pati, Superposition of causal order as a metrological resource for quantum thermometry, arXiv:1812.07508 (2018).
- [40] M. Frey, Indefinite causal order aids quantum depolarizing channel identification, *Quantum Inf Process* **18**, 96 (2019).
- [41] X. Zhao, Y. Yang, and G. Chiribella, Quantum Metrology with Indefinite Causal Order, *Phys. Rev. Lett.* **124**, 190503 (2020).
- [42] F. Chapeau-Blondeau, Noisy quantum metrology with the assistance of indefinite causal order, *Phys. Rev. A* **103**, 032615 (2021).
- [43] J. Wechs, H. Dourdent, A. A. Abbott, and C. Branciard, Quantum circuits with classical versus quantum control of causal order, *PRX Quantum* **2**, 030335 (2021).
- [44] J. Bavaresco, M. Murao, and M. T. Quintino, Strict Hierarchy between Parallel, Sequential, and Indefinite-Causal-Order Strategies for Channel Discrimination, *Phys. Rev. Lett.* **127**, 200504 (2021).
- [45] A (CS) strategy was shown to achieve super-Heisenberg scaling in a quantum metrology problem with infinite-dimensional systems [41]. This does not contradict our results, since in this work we derive bounds for finite-dimensional systems.
- [46] T. Uden, P. Balasubramanian, D. Louzon, Y. Vinkler, M. B. Plenio, M. Markham, D. Twitchen, A. Stacey, I. Lovchinsky, A. O. Sushkov, M. D. Lukin, A. Retzker, B. Naydenov, L. P. McGuinness, and F. Jelezko, Quantum metrology enhanced by repetitive quantum error correction, *Phys. Rev. Lett.* **116**, 230502 (2016).
- [47] R. Chaves, J. B. Brask, M. Markiewicz, J. Kołodyński, and A. Acín, Noisy metrology beyond the standard quantum limit, *Phys. Rev. Lett.* **111**, 120401 (2013).
- [48] C. W. Helstrom, *Quantum detection and estimation theory* (Academic press, 1976).
- [49] S. L. Braunstein and C. M. Caves, Statistical distance and the geometry of quantum states, *Phys. Rev. Lett.* **72**, 3439 (1994).
- [50] A. Fujiwara and H. Imai, A fibre bundle over manifolds of quantum channels and its application to quantum statistics, *J. Phys. A* **41**, 255304 (2008).
- [51] B. M. Escher, R. L. de Matos Filho, and L. Davidovich, General framework for estimating the ultimate precision limit in noisy quantum-enhanced metrology, *Nature Phys.* **7**, 406 (2011).
- [52] R. Demkowicz-Dobrzański, J. Kołodyński, and M. Guță, The elusive Heisenberg limit in quantum-enhanced metrology, *Nat. Commun.* **3**, 1063 (2012).
- [53] J. Kolodyński and R. Demkowicz-Dobrzański, Efficient tools for quantum metrology with uncorrelated noise, *New J. Phys.* **15**, 073043 (2013).
- [54] Similar philosophy may be found in [25, 34], yet the final results obtained there lacked either generality or tightness.
- [55] M. Szczykulska, T. Baumgratz, and A. Datta, Multi-parameter quantum metrology, *Advances in Physics: X* **1**, 621 (2016).
- [56] F. Albarelli and R. Demkowicz-Dobrzański, Probe incompatibility in multiparameter noisy quantum metrology, *Phys. Rev. X* **12**, 011039 (2022).
- [57] M. J. W. Hall and H. M. Wiseman, Heisenberg-style bounds for arbitrary estimates of shift parameters including prior information, *New J. Phys.* **14**, 033040 (2012).
- [58] J. Rubio and J. Dunningham, Bayesian multiparameter quantum metrology with limited data, *Phys. Rev. A* **101**, 032114 (2020).
- [59] Y. Matsuzaki, S. C. Benjamin, and J. Fitzsimons, Magnetic field sensing beyond the standard quantum limit under the effect of decoherence, *Phys. Rev. A* **84**, 012103 (2011).
- [60] A. W. Chin, S. F. Huelga, and M. B. Plenio, Quantum Metrology in Non-Markovian Environments, *Phys. Rev. Lett.* **109**, 233601 (2012).
- [61] A. Smirne, J. Kołodyński, S. F. Huelga, and R. Demkowicz-Dobrzański, Ultimate precision limits for noisy frequency estimation, *Phys. Rev. Lett.* **116**, 120801 (2016).
- [62] F. Beaudoin, L. M. Norris, and L. Viola, Ramsey interferometry in correlated quantum noise environments, *Phys. Rev. A* **98**, 020102(R) (2018).
- [63] S. Pirandola, R. Laurenza, C. Lupo, and J. L. Pereira, Fundamental limits to quantum channel discrimination, *npj Quantum Inf.* **5**, 50 (2019).
- [64] V. Katariya and M. M. Wilde, Geometric distinguishability measures limit quantum channel estimation and discrimination, *Quantum Inf Process* **20**, 78 (2021).
- [65] M. M. Wilde, M. Berta, C. Hirche, and E. Kaur, Amortized channel divergence for asymptotic quantum channel discrimination, *Lett Math Phys* **110**, 2277 (2020).
- [66] X. Wang and M. M. Wilde, Resource theory of asymmetric distinguishability for quantum channels, *Phys. Rev. Research* **1**, 033169 (2019).
- [67] K. Fang, O. Fawzi, R. Renner, and D. Sutter, Chain Rule for the Quantum Relative Entropy, *Phys. Rev. Lett.* **124**, 100501 (2020).
- [68] A. W. Harrow, A. Hassidim, D. W. Leung, and J. Watrous, Adaptive versus nonadaptive strategies for quantum channel discrimination, *Phys. Rev. A* **81**, 032339 (2010).
- [69] F. Salek, M. Hayashi, and A. Winter, Usefulness of adaptive strategies in asymptotic quantum channel discrimination, *Phys. Rev. A* **105**, 022419 (2022).
- [70] J. Bavaresco, M. Murao, and M. T. Quintino, Unitary channel discrimination beyond group structures: Advantages of sequential and indefinite-causal-order strategies, *J. Math. Phys.* **63**, 042203 (2022).
- [71] P. Sekatski and M. Perarnau-Llobet, Optimal nonequilibrium thermometry in Markovian environments, *Quantum* **6**, 869 (2022).

Appendix A: Optimal estimation strategies in case of the perpendicular dephasing model ($n = 2$).

Before presenting the analysis of the example, let us recall the definition of the QFI for completeness of the presentation. Given a parameter dependent state ρ_φ , the

corresponding QFI reads:

$$F(\rho_\varphi) = \text{Tr}(\rho_\varphi L_\varphi^2), \quad \frac{d\rho_\varphi}{d\varphi} = \frac{1}{2}(\rho_\varphi L_\varphi + L_\varphi \rho_\varphi), \quad (\text{A1})$$

where L_φ is the symmetric logarithmic derivative (SLD) and can be computed from the rightmost formula above. For pure states, the formula simplifies to

$$F(|\psi_\varphi\rangle) = 4 \left(\langle \dot{\psi}_\varphi | \dot{\psi}_\varphi \rangle - |\langle \dot{\psi}_\varphi | \psi_\varphi \rangle|^2 \right), \quad (\text{A2})$$

where $|\dot{\psi}_\varphi\rangle = \frac{d|\psi_\varphi\rangle}{d\varphi}$. Operationally, the inverse of the QFI provides a lower bound on the minimal achievable variance of the estimated parameter, via the quantum Cramér-Rao bound [48, 49], $\Delta^2 \tilde{\varphi} \geq 1/F$.

In particular for ideal phase encoding, where the phase is coherently imprinted k times on a balanced superposition state: $|\psi_\varphi\rangle = (|0\rangle + e^{ik\varphi}|1\rangle)/\sqrt{2}$, $F = k^2$. This implies, the result $F^{(1)} = 1$, for single use, $n = 1$, of the channel in the example discussed in the main text.

Given two uses of a channel, $n = 2$, and utilizing no entanglement or adaptiveness, the most straightforward strategy is to use the two channels independently, and send optimal single qubit probes to each of them. In this case we get the QFI $F_C^{(2)} = 2$ (twice the single-channel QFI).

This value may be improved by considering a parallel strategy involving an entangled input state $|\psi^{(2)}\rangle = (|00\rangle + |11\rangle)/\sqrt{2}$ (the N00N state), which results in the output state of the form:

$$\begin{aligned} \rho_{\varphi,E}^{(2)} &= \Lambda_\varphi^{\otimes 2} \left(|\psi^{(2)}\rangle \langle \psi^{(2)}| \right) = \\ & [p^2 + (1-p)^2] |\psi_\varphi^{(2)}\rangle \langle \psi_\varphi^{(2)}| + 2p(1-p) |\phi^{(2)}\rangle \langle \phi^{(2)}|, \end{aligned} \quad (\text{A3})$$

where $|\psi_\varphi^{(2)}\rangle = (|00\rangle + e^{2i\varphi}|11\rangle)/\sqrt{2}$, is the state corresponding to an effectively noiseless phase encoding (when two or none σ_x errors occur), while the orthogonal state $|\phi^{(2)}\rangle = (|01\rangle + |10\rangle)/\sqrt{2}$, contains no φ information (when one σ_x error occurred). As a result the QFI reads $F_E^{(2)} = (p^2 + (1-p)^2) \times 4 \geq 2$ —larger than when the two channels are used independently.

Interestingly, this result may be further improved via a simple adaptive strategy. The protocol involves entangling the initial single probe qubit with a single ancillary qubit in the same state as in the parallel strategy: $|\psi^{(2)}\rangle$. After a single action of the channel, $\lambda_\varphi \otimes \mathcal{I}$, an error correction operation is performed \mathcal{R} , where we check if a σ_x error occurred by projecting the state on one of the two subspaces $\mathcal{C} = \text{span}(|00\rangle, |11\rangle)$ and $\mathcal{E} = \text{span}(|10\rangle, |01\rangle)$, and correct the error accordingly. Afterwards, the second action of the channel is applied. The resulting state at the end of the protocol reads:

$$\begin{aligned} \rho_{\varphi,AD}^{(2)} &= (\Lambda_\varphi \otimes \mathcal{I}) \circ \mathcal{R} \circ (\Lambda_\varphi \otimes \mathcal{I}) \left(|\psi^{(2)}\rangle \langle \psi^{(2)}| \right) = \\ & p |\psi_\varphi^{(2)}\rangle \langle \psi_\varphi^{(2)}| + (1-p) |\phi^{(2)}\rangle \langle \phi^{(2)}|. \end{aligned} \quad (\text{A4})$$

This protocols yield $F_{AD}^{(2)} = 4p$ and is optimal provided $p \geq 0.5$. If $p < 0.5$, then one simply needs to modify the recovery operation in a way that instead of correcting a single σ_x error on the probe system the σ_x operation is applied to the ancillary qubit. This yields effectively $F_{AD}^{(2)} = 4(1-p)$. So in the end the optimal QFI reads $F_{AD}^{(2)} = 2(1 + |1 - 2p|)$, which is always larger than the parallel $F_E^{(2)}$ except for the $p = 0.5$ case when they are equal.

Having said that, it needs to be noticed that if we restrict ourselves to utilizing coherence only, we should in principle also allow a scenario where a single probe goes through the two channels sequentially. Consider $|+\rangle$ as an input (which is the optimal choice). As a result of going through the the two channels the output state reads:

$$\rho_{\varphi,C}^{(2)} = p |\psi_{2\varphi}\rangle \langle \psi_{2\varphi}| + (1-p) |+\rangle \langle +|. \quad (\text{A5})$$

This state looks very similar to the output state resulting from the adaptive strategy, Eq. (A4). Still, in Eq. (A4) we may perform a measurement that unambiguously discriminates between the ideally phase-encoded state, $|\psi_\varphi^{(2)}\rangle$, and the non-informative state $|\phi^{(2)}\rangle$. In case of Eq. (A5) this is no longer possible as the “signal” state $|\psi_{2\varphi}\rangle$ and non-informative $|+\rangle$ are not orthogonal in general and hence one cannot simply filter out the non-informative term. Indeed, direct computation of the QFI, using Eq. (A1), for the state $\rho_{\varphi,C}^{(2)}$ yields

$$F_C^{(2)} = 2p[1 + p + (1-p) \cos 2\varphi]. \quad (\text{A6})$$

While in general this value is smaller than $F_{AD}^{(2)}$, it approaches the performance of the adaptive scheme for $\varphi \approx 0$, and $p \geq 0.5$, $F_C^{(2)} \approx 4p$. This shows that sometimes even a basic sequential scheme (utilizing only coherence, and no adaptiveness) may be superior to the optimal entanglement-based scheme.

It should be pointed out, however, that for larger n the simple sequential strategy will quickly become ineffective due to a build-up of unchecked decoherence effects which cause the resulting QFI to be damped. In this regime, more advanced strategies are required (E), (AD) or (CS) in order to exploit the full potential of quantum enhanced sensing.

Appendix B: Operator norm inequality

Here we prove Eq. (7),

$$\left\| \sum_{k=1}^K L_k^\dagger A Q_k \right\| \leq \sqrt{\left\| \sum_{k=1}^K L_k^\dagger L_k \right\|} \|A\| \sqrt{\left\| \sum_{k=1}^K Q_k^\dagger Q_k \right\|}, \quad (\text{B1})$$

which is a key step in the derivation of the bounds. Let us introduce the following $K \times K$ block matrices:

$$\tilde{L} = \begin{bmatrix} L_1 & 0 & \dots & 0 \\ \vdots & \vdots & & \vdots \\ L_K & 0 & \dots & 0 \end{bmatrix}, \quad \tilde{Q} = \begin{bmatrix} Q_1 & 0 & \dots & 0 \\ \vdots & \vdots & & \vdots \\ Q_K & 0 & \dots & 0 \end{bmatrix}, \quad (\text{B2})$$

and $\tilde{A} = \mathbb{1}_{K \times K} \otimes A$. Note that

$$\tilde{L}^\dagger \tilde{A} \tilde{Q} = \begin{bmatrix} \sum_{k=1}^K L_k^\dagger A Q_k & 0 & \dots & 0 \\ \vdots & \vdots & & \vdots \\ 0 & 0 & \dots & 0 \end{bmatrix}. \quad (\text{B3})$$

This implies that:

$$\left\| \sum_{k=1}^K L_k^\dagger A Q_k \right\| = \left\| \tilde{L}^\dagger \tilde{A} \tilde{Q} \right\| \leq \|\tilde{L}^\dagger\| \|\tilde{A}\| \|\tilde{Q}\|, \quad (\text{B4})$$

where the inequality follows from the sub-multiplicativity property of the operator norm. Invoking now another operator norm property valid for arbitrary operators acting on a Hilbert space, $\|A\| = \sqrt{\|A^\dagger A\|}$ and $\|A^\dagger\| = \|A\|$, we get

$$\|\tilde{L}^\dagger\| \|\tilde{A}\| \|\tilde{Q}\| = \sqrt{\|\tilde{L}^\dagger \tilde{L}\|} \|\tilde{A}\| \sqrt{\|\tilde{Q}^\dagger \tilde{Q}\|}. \quad (\text{B5})$$

Finally, noticing that $\|\tilde{L}^\dagger \tilde{L}\| = \|\sum_k L_k^\dagger L_k\|$, $\|\tilde{A}\| = \|A\|$ and $\|\tilde{Q}^\dagger \tilde{Q}\| = \|\sum_k Q_k^\dagger Q_k\|$ we arrive at Eq. (B1).

Appendix C: Derivation of the bound for causal superposition strategies

For (CS) strategies, any quantum superposition of $n!$ possible causal orders of n elementary channels can be created. This can be achieved by entangling all different causal orders with an external, $n!$ -level quantum control system [35, 38]. As in (AD) strategies, we are allowed to put control unitaries between channels, moreover, for different causal orders, control unitaries may be different. Therefore, (AD) is a subclass of (CS), in which only one causal order of channels is probed. The channel describing the action of n elementary channels Λ in the superposition of different causal orders is $\Lambda_{\text{CS}}^{(n)}(\cdot) = \sum_{\mathbf{k}^{(n)}} K_{\mathbf{k}^{(n)}}^{\text{CS}} \cdot K_{\mathbf{k}^{(n)}}^{\text{CS}\dagger}$, where

$$K_{\mathbf{k}^{(n)}}^{\text{CS}} = \sum_{\pi \in \sigma(n)} K_{\mathbf{k}_{\pi}^{(n)}}^{\pi} \otimes |\pi\rangle \langle \pi|, \quad (\text{C1})$$

$\sigma(n)$ is the set of all n -element permutations, $\mathbf{k}_{\pi}^{(n)} = (k_{\pi(n)}, \dots, k_{\pi(1)})$. The Kraus operators $K_{\mathbf{k}^{(n)}}^{\pi}$ are defined iteratively, as in the adaptive case: $K_{\mathbf{k}^{(1)}}^{\pi} = V_1^{\pi}(K_{k_1} \otimes \mathbb{1})$,

$$K_{\mathbf{k}^{(i+1)}}^{\pi} = V_{i+1}^{\pi}(K_{k_{i+1}} \otimes \mathbb{1}) K_{\mathbf{k}^{(i)}}^{\pi}, \quad (\text{C2})$$

V_i^{π} is the control unitary applied after i -th channel when the order of channels is described by permutation π , $|\pi\rangle$ is a corresponding state of a control system.

The (CS) family of strategies has been studied in the context of quantum metrology in Ref. [35], where numerical values of the QFI were obtained for $n = 2$ and $n = 3$ (the Authors use abbreviation ‘‘sup’’ instead of ‘‘CS’’). Notice, that the formal definition of (CS) strategies from Appendix C.4 of Ref. [35] does not contain the explicit form of the channel $\Lambda_{\text{CS}}^{(n)}$. The explicit Kraus representation of a similar channel is present, for example, in [42] (for $n = 2$). The Choi-Jamiołkowski matrix of a channel involving superpositions of different causal orders for $n > 2$ is explicitly written down in [43].

Before we proceed further, let us show that we defined $\Lambda_{\text{CS}}^{(n)}$ in a way that does not depend on the choice Kraus representations of elementary channels Λ in (C2). Starting from an arbitrary Kraus representation $\{K_i\}$, we can construct any equivalent representation of the same channel $\{K'_j\}$ as $K'_j = \sum_i u_{ji} K_i$, where coefficients u_{ij} form a unitary matrix [50]. For a fixed π , the channel $\Lambda_{\pi}^{(n)}$, given by Kraus operators $K_{\mathbf{k}^{(n)}}^{\pi}$, is the concatenation of elementary channels Λ and unitary operations $V_1^{\pi}, V_2^{\pi}, \dots, V_n^{\pi} - \Lambda_{\pi}^{(n)}$ is well defined without referring to a particular Kraus representations of the elementary channel Λ . For this reason, changing the representation of each Λ may only change the Kraus operators $\{K_{\mathbf{k}^{(n)}}^{\pi}\}$ to an equivalent representation $\{K'_{\mathbf{l}^{(n)}}\}$, where $K'_{\mathbf{l}^{(n)}} = \sum_{\mathbf{k}^{(n)}} u_{\mathbf{l}^{(n)}, \mathbf{k}^{(n)}} K_{\mathbf{k}^{(n)}}^{\pi}$, the coefficients $u_{\mathbf{l}^{(n)}, \mathbf{k}^{(n)}}$ form a unitary matrix. Consequently, the Kraus operators $\{K_{\mathbf{k}^{(n)}}^{\text{CS}}\}$ transform to $\{K'_{\mathbf{l}^{(n)}}\}$, where

$$K'_{\mathbf{l}^{(n)}}^{\text{CS}} = \sum_{\pi \in \sigma(n)} \left(\sum_{\mathbf{k}^{(n)}} u_{\mathbf{l}^{(n)}, \mathbf{k}^{(n)}} K_{\mathbf{k}^{(n)}}^{\pi} \right) \otimes |\pi\rangle \langle \pi|. \quad (\text{C3})$$

This can be written as

$$K'_{\mathbf{l}^{(n)}}^{\text{CS}} = \sum_{\mathbf{k}^{(n)}} u_{\mathbf{l}^{(n)}, \mathbf{k}^{(n)}} K_{\mathbf{k}^{(n)}}^{\text{CS}}, \quad (\text{C4})$$

where

$$u_{\mathbf{l}^{(n)}, \mathbf{k}^{(n)}} = \sum_{\pi} u_{\mathbf{l}^{(n)}, \mathbf{k}^{(n)}}^{\pi} \otimes |\pi\rangle \langle \pi| \quad (\text{C5})$$

is a unitary matrix. Therefore, the Kraus operators $K'_{\mathbf{l}^{(n)}}^{\text{CS}}$ form an equivalent representation of a channel $\Lambda_{\text{CS}}^{(n)}$, so physical properties of this channel do not depend on the choice of representations of Λ .

In what follows, we derive an upper bound for the QFI achievable with any (CS) strategy involving n elementary channels, which can be efficiently computed for large n . We know that

$$F_{\text{CS}}^{(n)} \leq \min_{\{K_{\mathbf{k}^{(n)}}^{\text{CS}}\}} \left\| \alpha_{\text{CS}}^{(n)} \right\|, \quad \alpha_{\text{CS}}^{(n)} = \sum_{\mathbf{k}^{(n)}} \dot{K}_{\mathbf{k}^{(n)}}^{\text{CS}\dagger} \dot{K}_{\mathbf{k}^{(n)}}^{\text{CS}}, \quad (\text{C6})$$

where the minimization is taken over all Kraus representations of the channel $\Lambda_{\text{CS}}^{(n)}$. Such minimization is very hard to perform, but we can obtain a less tight but more feasible upper bound by minimizing over representations of a single channel only, assuming that the representation of each elementary channel Λ is the same:

$$F_{\text{CS}}^{(n)} \leq \min_{\{K_k\}} \left\| \alpha_{\text{CS}}^{(n)} \right\|. \quad (\text{C7})$$

For this family of representations, we have

$$\alpha_{\text{CS}}^{(n)} = \sum_{\mathbf{k}^{(n)}} \sum_{\pi \in \sigma^{(n)}} \dot{K}_{\mathbf{k}^{(n)}}^{\pi\dagger} \dot{K}_{\mathbf{k}^{(n)}}^{\pi} \otimes |\pi\rangle \langle \pi|. \quad (\text{C8})$$

The matrix $\alpha_{\text{CS}}^{(n)}$ has a block diagonal structure, where different blocks correspond to different π because the states $|\pi\rangle$ are orthogonal to each other. Therefore,

$$\left\| \alpha_{\text{CS}}^{(n)} \right\| = \max_{\pi \in \sigma^{(n)}} \left\| \sum_{\mathbf{k}^{(n)}} \dot{K}_{\mathbf{k}^{(n)}}^{\pi\dagger} \dot{K}_{\mathbf{k}^{(n)}}^{\pi} \right\|. \quad (\text{C9})$$

The summation inside a norm runs over all possible vectors $\mathbf{k}^{(n)}$, so it does not change when lower indices $\mathbf{k}_{\pi}^{(n)}$ are replaced with $\mathbf{k}^{(n)}$, so we have

$$\left\| \alpha_{\text{CS}}^{(n)} \right\| = \max_{\pi \in \sigma^{(n)}} \left\| \sum_{\mathbf{k}^{(n)}} \dot{K}_{\mathbf{k}^{(n)}}^{\pi\dagger} \dot{K}_{\mathbf{k}^{(n)}}^{\pi} \right\| \quad (\text{C10})$$

In this step, the assumption that the Kraus representations of all n elementary channels are the same, was crucial—otherwise, a different π would correspond to a different order of representations, so (C10) would not follow from (C9). That is why we cannot minimize over different representations for different channels, as we did for (AD) strategies, and the (CS) bound is less tight.

For a fixed π , the Kraus operators $K_{\mathbf{k}^{(n)}}^{\pi}$ describe an adaptive strategy on n elementary channels with control unitaries V_i^{π} . In (C10), maximization over π is equivalent to maximization over different sets of control unitaries V_i^{π} with a fixed causal order of channels, so we have

$$\left\| \alpha_{\text{CS}}^{(n)} \right\| \leq \max_{\{V_i\}} \left\| \sum_{\mathbf{k}^{(n)}} \dot{K}_{\mathbf{k}^{(n)}}^{\dagger} \dot{K}_{\mathbf{k}^{(n)}} \right\|, \quad (\text{C11})$$

where the maximization is over all sets of control unitaries, and $K_{\mathbf{k}^{(n)}}$ for a given $\{V_i\}$ are defined in (4). The upper bound for the r.h.s. for a fixed elementary channel representation $\{K_k\}$ is

$$\max_{\{V_i\}} \left\| \sum_{\mathbf{k}^{(n)}} \dot{K}_{\mathbf{k}^{(n)}}^{\dagger} \dot{K}_{\mathbf{k}^{(n)}} \right\| \leq a^{(n)}, \quad (\text{C12})$$

which follows directly from the derivation of the (AD) bound. Finally, we can minimize both sides of (C11)

and (C12) over $\{K_k\}$ to obtain

$$\min_{\{K_k\}} \left\| \alpha_{\text{CS}}^{(n)} \right\| \leq \min_{\{K_k\}} \max_{\{V_i\}} \left\| \sum_{\mathbf{k}^{(n)}} \dot{K}_{\mathbf{k}^{(n)}}^{\dagger} \dot{K}_{\mathbf{k}^{(n)}} \right\| \leq \min_{\{K_k\}} a^{(n)}. \quad (\text{C13})$$

This inequality, together with (C7), leads directly to the upper bound for $F_{\text{CS}}^{(n)}$ from (10).

The considered class of strategies (CS) is quite general, since it allows superpositions of all different causal orders of channels combined with all possible intermediate controls—moreover, for different causal orders, unitary controls may be different. However, quantum mechanics in principle allows for even more general non-causal strategies, the most general class of strategies is schematically shown in Fig. 1.e in Ref. [35], where the Authors refer to it using abbreviation ‘‘ICO’’. The advantage of (ICO) over (CS) strategies is usually very small, but possible to demonstrate numerically already for $n = 2$ [35]. Therefore, it is interesting to ask, whether our newly derived bound can be applied to the most general non-causal strategies (ICO). Unfortunately, the answer is negative, and a counterexample exists already for $n = 3$. Let us consider a single qubit channel studied in the *introductory example*, where noise is described by the Kraus operators from (1) with $p = 0.75$. For $n = 3$, exact values of the maximal QFI associated with (CS) and (ICO) strategies (obtained using procedures from [35]) are $F_{\text{CS}}^{(3)} = 5.52$, $F_{\text{ICO}}^{(3)} = 5.84$, whereas the upper bound for QFI for (CS) strategies is $\min_{\{K_k\}} 4a^{(3)} = 5.73$, so we have $F_{\text{CS}}^{(3)} < \min_{\{K_k\}} 4a^{(3)} < F_{\text{ICO}}^{(3)}$. Therefore, the problem of finding a feasible upper bound on the QFI for the most general non-causal strategies is still open. However, it is not clear whether all (ICO) strategies are possible to implement—probably this fundamental question should be addressed first.

Appendix D: Computing the iterative bounds

Firstly, let us describe more precisely the construction of the (AD) bound. When we construct $a^{(n)}$, defined in (9), we can choose the Kraus representation of the elementary channel $\{K_k\}$ independently in each step, so the norms $\|\alpha\|$, $\|\beta\|$ are different in each step. Then, we want to minimize $a^{(n)}$ over all possible sets of n representations $\{K_k\}^{\times n}$, the i -th element of such a set corresponds to the representation chosen in i -th step. However, $a^{(i+1)}$ depends only on $a^{(i)}$ and the representation chosen in the step $i + 1$, moreover, $a^{(i+1)}$ is an increasing function of $a^{(i)}$. Therefore, the minimum of $a^{(i+1)}$ over $\{K_k\}^{\times (i+1)}$ can be obtained by inserting the minimum of $a^{(i)}$ over $\{K_k\}^{\times i}$ into (9), and then minimizing the resulting expression over the representation of $(i + 1)$ -th channel.

As a result, the full optimization over n Kraus representations used in n steps may be easily obtained by performing n iterative optimizations over a single Kraus

representation in each successive step, namely:

$$\begin{aligned} \min_{\{K_k\}^{\times n}} a^{(n)} &= \tilde{a}^{(n)}, \quad \text{where } \tilde{a}^{(0)} = 0, \\ \tilde{a}^{(i+1)} &= \min_{\{K_k\}} \left[\tilde{a}^{(i)} + \|\alpha_{\{K_k\}}\| + 2\|\beta_{\{K_k\}}\| \sqrt{\tilde{a}^{(i)}} \right]. \end{aligned} \quad (\text{D1})$$

We used notation $\alpha_{\{K_k\}}$ and $\beta_{\{K_k\}}$ to indicate the dependence of an elementary channel representation $\{K_k\}$, over which we minimize in step $(i+1)$. We are now ready to demonstrate the numerical procedures for computing (AD) and (CS) bounds.

1. Minimizing $\|\alpha\|$ assuming $\|\beta\| \leq b$

Let us show how to formulate the following minimization problem

$$g(b) = \underset{\{K_k\}}{\text{minimize}} \|\alpha_{\{K_k\}}\| \quad (\text{D2})$$

$$\text{subject to } \|\beta_{\{K_k\}}\| \leq b \quad (\text{D3})$$

as an SDP. Firstly, as shown in [50, 52], we can significantly limit the class of Kraus representations over which we minimize. Starting from arbitrary $\{K_k\}$, it is enough to consider representations $\{\tilde{K}_k\}$ satisfying

$$\tilde{K}_k = K_k, \quad \dot{\tilde{K}}_k = \dot{K}_k - i \sum_j h_{kj} K_j \quad (\text{D4})$$

to obtain all possible values of $(\|\alpha\|, \|\beta\|)$ for a given channel Λ , the coefficients h_{kj} must form a hermitian matrix $h \in \text{Herm}(\mathbb{C}^{r \times r})$. We can replace the minimization over $\{K_k\}$ with a minimization over h in (D2). Following the path from [52, 53], let us construct the following matrices

$$A = \left(\begin{array}{c|ccc} \lambda \mathbb{1}_d & \dot{K}_1^\dagger & \dots & \dot{K}_r^\dagger \\ \hline \dot{K}_1 & & & \\ \vdots & & \mathbb{1}_{d-r} & \\ \dot{K}_r & & & \end{array} \right), \quad (\text{D5})$$

$$B = \left(\begin{array}{c|c} b \mathbb{1}_d & i \sum_{k=1}^r \dot{K}_k^\dagger K_k \\ \hline (i \sum_{k=1}^r \dot{K}_k^\dagger K_k)^\dagger & b \mathbb{1}_d. \end{array} \right) \quad (\text{D6})$$

It can be shown, using Schur's complement condition, that

$$A \succeq 0 \iff \lambda \geq \|\alpha_{\{\tilde{K}_k\}}\|, \quad B \succeq 0 \iff b \geq \|\beta_{\{\tilde{K}_k\}}\|. \quad (\text{D7})$$

Therefore, the constraint $B \succeq 0$ is equivalent to upper bounding $\|\beta\|$ by b , and minimization of λ is equivalent to minimization of $\|\alpha\|$. All elements of A and B are linear in λ and h , so we can use constraints for positivity of A and B in the SDP. All this observations allow us to write down the minimization problem (D2) as an SDP described in Algorithm 1.

Algorithm 1 Minimize $\|\alpha\|$ given $\|\beta\| \leq b$

Input: $K_k, \dot{K}_k \in \mathbb{C}^{d \times d}$ for $k \in \{1, \dots, r\}$ \triangleright Kraus operators of elementary channel Λ and their derivatives

Input: $b \geq 0$ \triangleright Upper bound for $\|\beta\|$

Output: $g(b) = \min_{\{K_k\}} \|\alpha\|$ s.t. $\|\beta\| \leq b$

- 1: variables: $\lambda \geq 0, h \in \text{Herm}(\mathbb{C}^{r \times r})$ \triangleright Variables to optimize in SDP
 - 2: **for** k in $(1, \dots, r)$ **do**
 - 3: $\dot{\tilde{K}}_k := \dot{K}_k - i \sum_{j=1}^r h_{kj} K_j$
 - 4: **end for**
 - 5: construct matrices A, B defined in (D5), (D6)
 - 6: minimize $_{\lambda, h}$ λ
subject to $A \succeq 0, B \succeq 0$ \triangleright SDP
 - 7: **Output** λ
-

2. Computing (AD) and (CS) bounds

Let us prove the following lemma:

Lemma 1 Let $f(x, y)$ be an increasing function of x and y with non-negative values. Then,

$$\min_{\{K_k\}} f(\|\alpha_{\{K_k\}}\|, \|\beta_{\{K_k\}}\|) = \min_{b \in [l, r]} f(g(b), b), \quad (\text{D8})$$

where $l = \min_{\{K_k\}} \|\beta_{\{K_k\}}\|$, $r = \min_{\{K_k\}} \sqrt{\|\alpha_{\{K_k\}}\|}$, $g(b)$ is defined in (D2).

Proof First note that

$$\begin{aligned} \min_{\{K_k\}} f(\|\alpha_{\{K_k\}}\|, \|\beta_{\{K_k\}}\|) &= \\ \min_{b \geq l} \min_{\{K_k: \|\beta_{\{K_k\}}\| \leq b} f(\|\alpha_{\{K_k\}}\|, b) &= \min_{b \geq l} f(g(b), b), \end{aligned} \quad (\text{D9})$$

where we used the fact that $f(x, y)$ is increasing with y (1st equality) and x (2nd equality). What remains to be proven is that the minimal value is always obtained for $b \leq r$. From (7), we have $\|\beta_{\{K_k\}}\| \leq \sqrt{\|\alpha_{K_k}\|}$, which means that $l \leq r$. Let $\{K'_k\}$ be the Kraus representation minimizing $\|\alpha\|$, which means that $\sqrt{a'} = \sqrt{\|\alpha_{\{K'_k\}}\|} = r$, $b' = \|\beta_{\{K'_k\}}\| \leq \sqrt{\|\alpha_{\{K'_k\}}\|} = r$. Obviously, $a' \leq a$, so when we choose $\{K_k\}$ such that $b > r$, we have $a' \leq a$ and $b' = r < b$, so $f(a', b') < f(a, b)$, which means that the minimum cannot be achieved for $b > r$. ■

The values of l and r can be found using an SDP, as described in [52, 53]—the result of a minimization of λ with the constraint $A \succeq 0$ is r^2 , and the minimum of b with the constraint $B \succeq 0$ equals to l .

Notice, that $\tilde{a}^{(i+1)}$ defined in (D1) is an increasing function of $\|\alpha\|$ and $\|\beta\|$, so we can use Lemma 1 to perform the minimization over $\{K_k\}$:

$$\tilde{a}^{(i+1)} = \min_{b \in [l, r]} \left[\tilde{a}^{(i)} + g(b) + 2b\sqrt{\tilde{a}^{(i)}} \right] \quad (\text{D10})$$

In practice, we do not have an analytical form of $g(b)$, and we need to solve an SDP problem for each argument

b independently to obtain $g(b)$. Therefore, minimization over $b \in [l, r]$ is approximated with minimization over $b \in \text{Linspace}(l, r, p)$, where $\text{Linspace}(l, r, p)$ is a p -element arithmetic sequence whose first element is l and last element is r . Notice, that this approximation can only increase the final result—therefore, even for small sampling precision p , we obtain valid, but not necessary tight, upper bounds. We used the value $p = 500$ to generate the data presented in this paper, further precision increase did not lead to any significant difference.

To sum up, the procedure to compute the upper bound for $F_{\text{AD}}^{(n)}$ is as follows. Firstly, we compute l and r using the SDP. Secondly, $g(b)$ is calculated for $b \in \text{Linspace}(l, r, p)$. Finally, we initialize $\tilde{a}^{(0)} = 0$, and compute $\tilde{a}^{(i)}$ for larger i iteratively using (D1). Notice, that the computational cost of each iteration is very low since we computed all the required values of $g(b)$ at the beginning, and we keep them in the memory. The computation of $g(b)$ for p different values of b is the most time-consuming part, but even for a high precision ($p = 500$), the computation time did not exceed two minutes. Once we do this computation, we can easily get an upper bound for $F_{\text{AD}}^{(n)}$ even for large values of n .

The procedure to compute an upper bound for $F_{\text{CS}}^{(n)}$ is very similar. Notice, that $a^{(i)}$ defined in (9) is an increasing function of $\|\alpha\|$ and $\|\beta\|$, so we can use Lemma 1 to find its minimum over a single $\{K_k\}$:

$$\begin{aligned} \min_{\{K_k\}} a^{(n)} &= \min_{b \in [l, r]} \hat{a}^{(n)}(b) \quad , \text{ where } \hat{a}^{(0)}(b) = 0, \\ \hat{a}^{(i+1)}(b) &= \hat{a}^{(i)}(b) + g(b) + 2b\sqrt{\hat{a}^{(i)}(b)} \end{aligned} \quad (\text{D11})$$

Subsequent values of $\hat{a}^{(i)}(b)$ are found iteratively for all $b \in \text{Linspace}(l, r, p)$, and then minimization over b is performed with the help of previously calculated values of $g(b)$. The whole procedure of computing bounds for $F_{\text{AD}}^{(n)}$ and $F_{\text{CS}}^{(n)}$ is summarized in Algorithm 2.

Algorithm 2 Iterative bounds for $F_{\text{AD}}^{(n)}$ and $F_{\text{CS}}^{(n)}$

Input: $K_k, \hat{K}_k \in \mathbb{C}^{d \times d}$ for $k \in \{1, \dots, r\}$
Input: $n \in \mathbb{Z}_+$ ▷ Max number of elementary channels
Input: $p \in \mathbb{Z}_+$ ▷ Precision of sampling
Output: AD, CS: lists of size n , AD/CS[k] is an upper bound for $F_{\text{AD/CS}}^{(k)}$

- 1: $l := \min_{\{K_k\}} \|\beta\|$
- 2: $r := \min_{\{K_k\}} \sqrt{\|\alpha\|}$
- 3: variables: $a[p], b[p], t1[p], t2[p], \text{AD}[n], \text{CS}[n]$ ▷ Lists of real numbers of size $[]$, initialized with 0s
- 4: $b := \text{Linspace}(l, r, p)$ ▷ $b[1] = l, b[p] = r, b[1], b[2], \dots, b[p]$ is arithmetic sequence
- 5: **for** j in $(1, \dots, p)$ **do**
 $a[j] := g(b[j])$ ▷ Use Alg. 1
- 6: **end for**
 ▷ Computing AD bounds
- 7: $m := 0$
- 8: **for** k in $(1, \dots, n)$ **do**
- 9: **for** j in $(1, \dots, p)$ **do**
- 10: $t1[j] := m + a[j] + 2 * b[j] * \sqrt{m}$
- 11: **end for**
- 12: $m := \text{Minimum}[t1]$
- 13: $\text{AD}[k] := 4 * m$
- 14: **end for**
 ▷ Computing CS bounds
- 15: **for** k in $(1, \dots, n)$ **do**
- 16: **for** j in $(1, \dots, p)$ **do**
- 17: $t2[j] := t2[j] + a[j] + 2 * b[j] * \sqrt{t2[j]}$
- 18: **end for**
- 19: $\text{CS}[k] := 4 * \text{Minimum}[t2]$
- 20: **end for**
- 21: **Output** AD, CS

The old bound for (AD) strategies can be also computed numerically using Lemma 1—the minimization from (3) simplifies to:

$$\begin{aligned} \min_{\{K_i\}} 4 \left[n\|\alpha\| + n(n-1)\|\beta\| \left(\|\beta\| + 2\sqrt{\|\alpha\|} \right) \right] &= \\ \min_{b \in [l, r]} 4 \left[ng(b) + n(n-1)b(b + 2\sqrt{g(b)}) \right]. \end{aligned} \quad (\text{D12})$$

Analogously, we can compute the new analytical bound from (12), or the bound for (E) strategies (2). Therefore, the function $g(b)$ fully characterizes an elementary channel Λ_φ from a metrological point of view—if we know $g(b)$ (at least for some values of b), we can easily compute all metrological bounds.

3. Tightening of the bound for parallel strategies

Looking at the original derivation of the bound for parallel strategies in [50], we see that it may be tightened by allowing different Kraus representations for each elementary Hilbert space in Eq. (16) of [50]. However, the full optimization here is a bit more complicated to perform than in the adaptive case, while the advantage over the standard parallel bound (2) is not significant for the

typical examples (what we checked numerically). Still, it is worth noting that such an optimized bound is guaranteed to be tighter than the newly derived adaptive one (10), which we show below.

The channel describing the parallel action of n elementary channels Λ is $\Lambda_{\mathbf{E}}^{(n)}(\cdot) = \sum_{\mathbf{k}^{(n)}} K_{\mathbf{k}^{(n)}}^{\mathbf{E}} \cdot K_{\mathbf{k}^{(n)}}^{\mathbf{E}\dagger}$, where $K_{\mathbf{k}^{(1)}}^{\mathbf{E}} = K_{k_1} \otimes \mathbb{1}$,

$$K_{\mathbf{k}^{(i+1)}}^{\mathbf{E}} = K_{k_{i+1}} \otimes K_{\mathbf{k}^{(i)}}^{\mathbf{E}}, \quad (\text{D13})$$

$\mathbb{1}$ is acting on an ancillary system. Using this definition, we obtain the following iteration relations for $\alpha_{\mathbf{E}}^{(n)} = \sum_{\mathbf{k}^{(n)}} \dot{K}_{\mathbf{k}^{(n)}}^{\mathbf{E}\dagger} \dot{K}_{\mathbf{k}^{(n)}}^{\mathbf{E}}$, $\beta_{\mathbf{E}}^{(n)} = \sum_{\mathbf{k}^{(n)}} \dot{K}_{\mathbf{k}^{(n)}}^{\mathbf{E}\dagger} K_{\mathbf{k}^{(n)}}^{\mathbf{E}}$:

$$\alpha_{\mathbf{E}}^{(i+1)} = \alpha \otimes \mathbb{1} + \mathbb{1} \otimes \alpha_{\mathbf{E}}^{(i)} - 2\beta \otimes \beta_{\mathbf{E}}^{(i)}, \quad (\text{D14})$$

$$\beta_{\mathbf{E}}^{(i+1)} = \beta \otimes \mathbb{1} + \mathbb{1} \otimes \beta_{\mathbf{E}}^{(i)}, \quad (\text{D15})$$

$\mathbb{1}$ acting on an ancillary system was omitted. From the triangle inequality:

$$\|\alpha_{\mathbf{E}}^{(i+1)}\| \leq \|\alpha_{\mathbf{E}}^{(i)}\| + \|\alpha\| + 2\|\beta\| \|\beta_{\mathbf{E}}^{(i)}\|, \quad (\text{D16})$$

$$\|\beta_{\mathbf{E}}^{(i+1)}\| \leq \|\beta_{\mathbf{E}}^{(i)}\| + \|\beta\|. \quad (\text{D17})$$

Let us define

$$a_{\mathbf{E}}^{(i+1)} = a_{\mathbf{E}}^{(i)} + \|\alpha\| + 2\|\beta\| b_{\mathbf{E}}^{(i)}, \quad (\text{D18})$$

$$b_{\mathbf{E}}^{(i+1)} = b_{\mathbf{E}}^{(i)} + \|\beta\|, \quad a_{\mathbf{E}}^{(0)} = 0, \quad b_{\mathbf{E}}^{(0)} = 0. \quad (\text{D19})$$

Using the inequality $\|\alpha_{\mathbf{E}}^{(n)}\| \leq a_{\mathbf{E}}^{(n)}$, we obtain the upper bound for the QFI associated with (E) strategies

$$F_{\mathbf{E}}^{(n)} \leq \min_{\{K_k\}} 4a_{\mathbf{E}}^{(n)}, \quad (\text{D20})$$

which is equivalent to the state-of-the-art bound presented in (2). Again, to make this bound tighter, we can allow for different Kraus representations of an elementary channel in each step of the iteration:

$$F_{\mathbf{E}}^{(n)} \leq \min_{\{K_k\}^{\times n}} 4a_{\mathbf{E}}^{(n)}. \quad (\text{D21})$$

From the inequality $\|\beta\|^2 \leq \|\alpha\|$ and from the induction principle follows $b_{\mathbf{E}}^{(i)} \leq \sqrt{a_{\mathbf{E}}^{(i)}}$. Therefore, if we compare (9) with (D18), we see that $a_{\mathbf{E}}^{(n)} \leq a^{(n)}$, so the iterative bound for (E) strategies is tighter than the one for (AD) strategies. However, the minimization from (D21) cannot be performed step by step as easily as in the adaptive case because the minimal value of $a_{\mathbf{E}}^{(i+1)}$ is not always achieved for the minimal value of $a_{\mathbf{E}}^{(i)}$.

Appendix E: Asymptotic equivalence between adaptive and parallel strategies

For any fixed single-channel Kraus representation $\{K_k\}$ (not necessarily the optimal one), we have:

$$a^{(i+1)} = a^{(i)} + \|\alpha\| + 2\|\beta\| \sqrt{a^{(i)}}, \quad a^{(0)} = 0. \quad (\text{E1})$$

We will show that $\forall_{n \geq 1} a^{(n)} \leq f(n)$, where:

$$f(n) = n\|\alpha\| + n(n-1)\|\beta\|^2 + n \log n (\|\alpha\| - \|\beta\|)^2. \quad (\text{E2})$$

First note that they are equal at $n = 1$:

$$f(1) = a^{(1)} = \|\alpha\|. \quad (\text{E3})$$

Next, we will show that this function satisfies the iteration rule (E1) with inequality \geq instead of $=$,

$$f(n+1) - f(n) \stackrel{?}{\geq} \|\alpha\| + 2\|\beta\| \sqrt{f(n)} \quad (\text{E4})$$

which would lead to $f(n) \geq a^{(n)}$.

To prove (E4), let us write down the l.h.s. explicitly:

$$f(n+1) - f(n) = \|\alpha\| + 2\|\beta\|^2 n + (\|\alpha\| - \|\beta\|)^2 ((1+n) \log(1+n) - n \log(n)). \quad (\text{E5})$$

Note that first derivative of $x \log(x)$ is a strictly increasing function, and therefore:

$$(1+n) \log(1+n) - n \log(n) = \int_n^{n+1} (x \log(x))' dx \geq (x \log(x))' \Big|_{x=n} = 1 + \log(n). \quad (\text{E6})$$

Using (E6), we can deduce that (E4) follows from

$$\|\alpha\| + 2\|\beta\|^2 n + (\|\alpha\| - \|\beta\|)^2 (1 + \log(n)) \stackrel{?}{\geq} \|\alpha\| + 2\|\beta\| \sqrt{\|\beta\|^2 n(n-1) + n\|\alpha\| + (\|\alpha\| - \|\beta\|)^2 n \log(n)}, \quad (\text{E7})$$

which, after subtracting $\|\alpha\|$, taking the square and subtracting the r.h.s. reduces to

$$(\|\alpha\| - \|\beta\|^2)^2 (1 + \log(n))^2 \geq 0, \quad (\text{E8})$$

which is always true.

Now, as $f(n) \geq a^{(n)}$ for any fixed Kraus representation, $4f(n)$ minimized over all Kraus representations constitutes a valid bound for the QFI (12).

Appendix F: Continuous time limit for Markovian dynamics

We consider a Markovian semigroup dynamics in continuous time, described by the Gorini-Kossakowski-Sudarshan-Lindblad (GKSL) master equation

$$\frac{d\rho}{dt} = -i[H, \rho] + \sum_{j=1}^J L_j \rho L_j^\dagger - \frac{1}{2} \rho L_j^\dagger L_j - \frac{1}{2} L_j^\dagger L_j \rho. \quad (\text{F1})$$

A Kraus representation of the dynamical map at the lowest order in Δt is

$$K_0 = \mathbb{1} - \left(iH + \frac{1}{2} \mathbf{L}^\dagger \mathbf{L} \right) \Delta t + O(\Delta t^2) \quad (\text{F2})$$

$$\mathbf{K} = \mathbf{L} \sqrt{\Delta t} + O(\Delta t^{\frac{3}{2}}), \quad (\text{F3})$$

where we introduced a vector notation $\mathbf{L} = [L_1, \dots, L_J]^T$ for the J collapse operators, which means $\mathbf{L}^\dagger \mathbf{L} = \sum_{j=1}^J L_j^\dagger L_j$, and for the J Kraus operators $\mathbf{K} = [K_1, \dots, K_J]^T$ (the 0th operator is kept separate). Following Refs. [22, 31], we obtain the continuous time evolution as the limit $\Delta t \rightarrow 0$ of repeated sequential applications of the channel with the above Kraus representation.

Since $F^{(i)} = 4\|\alpha^{(i)}\|$ when the input state involves ancillary systems [50], we can rewrite Eq. (8) as an inequality for the difference quotient of the (ancilla-assisted) QFI

$$\frac{F^{(i+1)} - F^{(i)}}{\Delta t} \leq \frac{4}{\Delta t} \left(\|\alpha\| + \|\beta\| \sqrt{F^{(i)}} \right), \quad (\text{F4})$$

where α and β depend on Δt through the Kraus operators in Eqs. (F2,F3).

The parameter φ to be estimated is arbitrary and can appear both in the Hamiltonian H and in the collapse operators L_j . The derivatives of the Kraus operators are

$$\dot{K}_0 = - \left(i\dot{H} + \frac{1}{2}\dot{\mathbf{L}}^\dagger \mathbf{L} + \frac{1}{2}\mathbf{L}^\dagger \dot{\mathbf{L}} \right) \Delta t \quad (\text{F5})$$

$$\dot{\mathbf{K}} = \dot{\mathbf{L}} \sqrt{\Delta t}. \quad (\text{F6})$$

The different Δt -order of the 0th Kraus operator suggests to divide the matrix h in Eq. (D4) that specifies the Kraus representations in blocks as

$$h = \begin{bmatrix} h_{00} & \mathbf{h}^\dagger \\ \mathbf{h} & \mathfrak{h} \end{bmatrix}, \quad (\text{F7})$$

with $h_{00} \in \mathbb{R}$ and $\mathfrak{h}^\dagger = \mathfrak{h}$. We expand this matrix in powers of Δt as follows

$$h = h^{(0)} + h^{(\frac{1}{2})} \sqrt{\Delta t} + h^{(1)} \Delta t, \quad (\text{F8})$$

and it must be chosen such that the limit for $\Delta t \rightarrow 0$ remains finite and Eq. (F4) gives a meaningful bound on the time-derivative of the QFI. From Eq. (F4) it is evident that we need to choose h such that the terms of order less than Δt in α and β are zero, while the terms of higher order become irrelevant in the limit $\Delta t \rightarrow 0$.

After some algebra one realizes that we must impose $h_{00}^{(0)} = h_{00}^{(\frac{1}{2})} = 0$ and $\mathbf{h}^{(0)} = 0$ to have $\beta^{(0)} = \beta^{(\frac{1}{2})} = \alpha^{(0)} = \alpha^{(\frac{1}{2})} = 0$; the first-order terms that remain rele-

vant in the limit are

$$\begin{aligned} -i\beta^{(1)} = & \dot{H} - \frac{i}{2} \left(\dot{\mathbf{L}}^\dagger \mathbf{L} - \mathbf{L}^\dagger \dot{\mathbf{L}} \right) + h_{00}^{(1)} \mathbb{1} + \mathbf{L}^\dagger \mathbf{h}^{(\frac{1}{2})} + \mathbf{h}^{(\frac{1}{2})\dagger} \mathbf{L} \\ & + \mathbf{L}^\dagger \mathfrak{h}^{(0)} \mathbf{L} \end{aligned} \quad (\text{F9})$$

and

$$\alpha^{(1)} = \left[\mathbf{h}^{(\frac{1}{2})} \mathbb{1} + \mathfrak{h}^{(0)} \mathbf{L} + i\dot{\mathbf{L}} \right]^\dagger \left[\mathbf{h}^{(\frac{1}{2})} \mathbb{1} + \mathfrak{h}^{(0)} \mathbf{L} + i\dot{\mathbf{L}} \right]. \quad (\text{F10})$$

The bound on the rate of increase of the QFI is

$$\frac{dF(t)}{dt} \leq 4 \min_{h_{00}^{(1)}, \bar{h}^{(\frac{1}{2})}, \mathfrak{h}^{(0)}} \left(\|\alpha^{(1)}\| + \|\beta^{(1)}\| \sqrt{F(t)} \right). \quad (\text{F11})$$

Since Eq. (8) can also be derived when a different channel is applied at each step, the previous inequality also holds in the Markovian time-inhomogenous case with time-dependent H and L_j in Eq. (F1).

Recently, the authors of Ref. [25] derived a bound tighter than the one in Refs. [22, 28], without relying on a discretization of the time evolution. For a Hamiltonian parameter (i.e. $\dot{\mathbf{L}} = 0$), Eq. (18) of Ref. [25] gives a state-dependent bound for arbitrary initial states. The inequalities in Eq. (19) of Ref. [25] can further be applied to obtain a state-independent bound for finite-dimensional systems which coincides with the bound in Eq. (F11) by applying the substitutions $-i\beta^{(1)} \leftrightarrow G$, $\alpha^{(1)} \leftrightarrow \sum_j A_j^\dagger A_j$, $h_{00}^{(1)} \leftrightarrow -x$, $h_j^{(\frac{1}{2})} \leftrightarrow -\beta_j$ and $\mathfrak{h}_{ij}^{(0)} \leftrightarrow -\gamma_{ij}$.

For a Hamiltonian parameter, the two asymptotic cases are

1. The Hamiltonian derivative \dot{H} is in the Lindblad span and we can find h such that $\beta^{(1)} = 0$ leading to

$$F \leq 4t \min_{h_{00}^{(1)}, \bar{h}^{(\frac{1}{2})}, \mathfrak{h}^{(0)}, \beta^{(1)}=0} \|\alpha^{(1)}\| \quad (\text{F12})$$

2. The Hamiltonian derivative \dot{H} is not in the Lindblad span, then the asymptotic solution of the differential equation for large t gives

$$F \leq 4t^2 \min_{h_{00}^{(1)}, \bar{h}^{(\frac{1}{2})}, \mathfrak{h}^{(0)}} \|\beta^{(1)}\|^2. \quad (\text{F13})$$

Both bounds are asymptotically attainable with the parallel strategies described in Refs. [28, 36]. However, Eq. (F11) can give tighter bounds for short times [25]. Finally, while the estimation of a parameter appearing in the collapse operators is less studied, the bounds of Refs. [22, 28] have recently been applied to study optimal quantum thermometry in Markovian environments [71], thus these tighter bounds may also be useful in that context.